Three-Dimensional Zinc Phosphates with Open Architectures

S. Neeraj and Srinivasan Natarajan*

Chemistry and Physics of Materials Unit, Jawaharlal Nehru Centre for Advanced Scientific Research, Jakkur P.O., Bangalore 560 064, India

Received April 5, 2000. Revised Manuscript Received June 20, 2000

Two new zinc phosphates, $[C_3N_2H_{12}]_2[Zn_4(PO_4)_4]$, **I**, $[C_3N_2H_{12}]_2[Zn_5(H_2O)(PO_4)_4(HPO_4)]$, **II**, have been synthesized hydrothermally in the presence of 1,3-diaminopropane (DAP). Both **I** and **II** consist of the vertex linking ZnO_4 and PO_4 tetrahedral units forming channels bound by eight T atoms (T = Zn, P). The structure of **II** possesses similar building units as that of the naturally occurring aluminosilicate mineral, thomsonite, but interruptions in the connectivity between the building units creates marginal differences. To our knowledge, **II** is the first analogue of thomsonite. The amine molecules, in **I** and **II**, are situated within the channels and the loss of the amine molecule causes the collapse of the framework forming condensed zinc phosphates. Crystal data: $[NH_3(CH_2)_3NH_3]_2[Zn_4P_4O_{16}]$ (**I**), M = 793.6, monoclinic, space group = $P2_1$ (no. 4), a = 10.200(1), b = 9.998(1), c = 10.447(1) Å, β = 92.24(1)°, V = 1064.62(3) Å^3, Z = 2, ρ_{calc} = 2.476 g cm^{-3}, μ(Mo Kα) = 4.840 mm^{-1}, R_1 = 0.038, wR_2 = 0.099 [2231 observed reflections with $I > 2\sigma(I)$]; $[C_3N_2H_{12}]_2[Zn_5(H_2O)(PO_4)_4(HPO_4)]$ (**II**), M = 973.02, monoclinic, space group = $P2_1$ (no. 4), a = 9.299(4), b = 9.751(1), c = 14.335(1) Å, β = 90.97(4)°, V = 1299.67(9) Å^3, Z = 2, ρ_{calc} = 2.486 g cm^{-3}, μ(MoKα) = 4.955 mm^{-1}, R_1 = 0.028, wR_2 = 0.063 [3389 observed reflections with $I > 2\sigma(I)$].

Introduction

A large number of open-framework metal phosphates have been synthesized and characterized in recent years. The interest in these materials is largely based on their potential applications in the areas of catalysis, sorption, and separation processes.[1] Of the various families of open-framework materials that have been synthesized,[2] the nickel phosphate, VSB-1,[3] and the zinc phosphate, ND-1,[4] are interesting for their large one-dimensional 24-membered channels. A survey of the available literature reveals that the zinc phosphates constitute the second largest family of open-framework materials that have been studied during the past few years.[4−13] This is not surprising considering that the bivalent metal (Zn) phosphates (+2 and +5) are associated with the same total charge as the aluminosilicate zeolites (+3 and +4). Several of the zinc phosphates possess zeolitic structures.[9a,b] In addition, zinc phosphates with zero- (monomer),[5] one- (chain, ladder),[6] two- (layer),[7] and three-dimensional[4,8−13] architectures have also been isolated in the presence of amine molecules employing hydrothermal methods. It is observed that in some zinc phosphates, the amine molecules are bound to Zn centers and act as a ligand in addition to being the structure-directing agent.[13] During our investigations on the synthesis of novel zinc phosphates, we have discovered two new materials possessing channels

* Corresponding author. E-mail: raj@jncasr.ac.in.

(1) Thomas, J. M. *Angew. Chem., Int. Ed.* **1999**, *38*, 3588 and references therein.

(2) Cheetham, A. K.; Ferey, G.; Loiseau, T. *Angew. Chem., Int. Ed.* **1999**, *39*, 3268 and references therein.

(3) Guillou, N.; Gao, Q.; Nogies, M.; Morris, R. E.; Herview, M.; Ferey, G.; Cheetham, A. K. *C. R. Acad. Sci. Paris Ser. II* **1999**, 387.

(4) Yang, G.-Y.; Sevov, S. C. *J. Am. Chem. Soc.* **1999**, *121*, 8389.

(5) Neeraj, S.; Natarajan, S.; Rao, C. N. R. *J. Solid State Chem.* **2000**, *150*, 417.

(6) (a) Rao, C. N. R.; Natarajan, S.; Neeraj, S. *J. Am. Chem. Soc.* **2000**, *122*, 2810. (b) Chidambaram, D.; Neeraj, S.; Natarajan, S.; Rao, C. N. R. *J. Solid State Chem.* **1999**, *147*, 154. (c) Harrison, W. T. A.; Bircsak, Z.; Hannoman, L.; Zhang, Z. J. *Solid State Chem.* **1998**, *136*, 93. Reinert, P.; Zabukovec, N.; Patarin, J.; Kaucic, V. *Eur. J. Solid State Inorg. Chem.* **1998**, *35*, 373.

(7) (a) Neeraj, S.; Natarajan S.; Rao, C. N. R. *Chem. Mater.* **1999**, *11*, 1390. (b) Neeraj, S.; Natarajan, S. *Int. J. Inorg. Mater.* **1999**, *1*, 317. (c) Harrison, W. T. A.; Phillips, M. L. F.; Clegg, W.; Teat, S. J. *J. Solid State Chem.* **1999**, *148*, 433 and references therein.

(8) (a) Song, T.; Hurshouse, M. B.; Chen, J.; Xu, J.; Malik, K. M. A.; Jones, R. H.; Xu R.; Thomas, J. M. *Adv. Mater.* **1994**, *6*, 679. (b) Liu, Y.; Na, L.; Zhu, G.; Xio, F.-S.; Pang, W.; Xu, R. *J. Solid State Chem.* **2000**, *149*, 107. (c) Harrison, W. T. A.; Martin, T. E.; Gier, T. E.; Stucky, G. D. *J. Mater. Chem.*, **1992**, *2*, 175. (d) Harrison, W. T. A.; Nenoff, T. M.; Gier, T. E.; Stucky, G. D. *Inorg. Chem.* **1992**, *31*, 5395.

(9) (a) Feng, P.; Bu X.; Stucky, G. D. *Angew. Chem., Int. Ed. Engl.* **1995**, *34*, 1745. (b) Gier, T. E.; Stucky, G. D. *Nature* **1991**, *349*, 508. (c) Feng, P.; Bu X.; Stucky, G. D. *J. Solid State Chem.* **1996**, *125*, 243. (d) Bu, X.; Feng, P.; Gier, T. E.; Stucky, G. D. *Zeolites* **1997**, *19*, 2000.

(10) (a) Harrison, W. T. A.; Gier, T. E.; Moran, K. L.; Eckert, H.; Stucky, G. D. *Chem. Mater.* **1991**, *3*, 27. (b) Nenoff, T. M.; Harrison, W. T. A.; Gier, T. E.; Stucky, G. D. *J. Am. Chem. Soc.* **1991**, *113*, 378. (c) Borach, R. W.; Bedard, R. A.; Song, S. G.; Pluth, J. J.; Bram, A.; Riekel, C.; Weber, H.-P. *Chem. Mater.* **1999**, *11*, 2076. (d) Harrison, W. T. A.; Nenoff, T. M.; Gier, T. E.; Stucky, G. D. *Inorg. Chem.* **1993**, *32*, 2437.

(11) (a) Harrison, W. T. A.; Philips, M. L. F. *Chem. Mater.* **1997**, *9*, 1837. (b) Harrison W. T. A.; Hannooman, L. *Angew. Chem., Int. Ed. Engl.* **1997**, *36*, 640. (c) Harrison, W. T. A.; Dussak L. L.; Jacobson, A. J. *J. Solid State Chem.* **1996**, *125*, 134; Harrison, W. T. A.; Broach, R. W.; Bedard, R. A.; Gier, T. W.; Bu, X.; Stucky, G. D. *Chem. Mater.* **1996**, *8*, 691.

(12) (a) Chidambaram D.; Natarajan, S. *Mater. Res. Bull.* **1998**, *33*, 1275. (b) Neeraj, S.; Natarajan, S.; Rao, C. N. R. *Chem. Commun.* **1999**, 165.

(13) (a) Neeraj, S.; Natarajan, S.; Rao, C. N. R. *New J. Chem.* **1999**, *23*, 303. (b) Vaidhyanathan, R.; Natarajan, S.; Rao, C. N. R. *J. Mater. Chem.* **1999**, *9*, 2789. (c) Harrison, W. T. A.; Nenoff, T. M.; Eddy, M. M.; Martin, T. E.; Stucky, G. D. *J. Mater. Chem.* **1992**, *2*, 1127.

10.1021/cm000283u CCC: $19.00
Published on Web 08/22/2000

bound by eight T atoms (T = Zn, P). In this paper, we report the synthesis and structures of **I**, $[C_3N_2H_{12}]_2[Zn_4(PO_4)_4]$, and **II**, $[C_3N_2H_{12}]_2[Zn_5(H_2O)(PO_4)_4(HPO_4)]$, possessing channels. **II** is closely related to the naturally occurring mineral, thomsonite.[14] This is the first report, to our knowledge, of a thomsonite analogue among zinc phosphates.

Experimental Section

Synthesis and Initial Characterization. Compounds **I** and **II** were synthesized under hydrothermal conditions using 1,3-diaminopropane (DAP). In a typical synthesis of **I**, 0.548 g of zinc acetate dihydrate ($Zn(ac)_2{\cdot}2H_2O$) was dispersed in a mixture containing 4.5 mL of deionized water and 0.22 mL of HCl (35%). To this 0.81 mL of phosphoric acid (85 wt %) was added under constant stirring. To this solution was added 1.26 mL of DAP, and the whole solution was stirred for 30 min. The final homogenized mixture was transferred in a PTFE-lined stainless steel autoclave and heated at 165 °C for 24 h. The final composition of the mixture was $Zn(ac)_2{\cdot}2H_2O$: $5H_3PO_4$:HCl:6DAP:$100H_2O$. The initial mixture had a pH of ~4. The resulting product predominantly contained large quantities of colorless truncated octahedron-like crystals. **II** was synthesized by employing an identical procedure, but with a composition of $Zn(ac)_2{\cdot}2H_2O$: $5H_3PO_4$:HCl:6DAP:$100H_2O$, which resulted in colorless rectangular thick platelike crystals. The crystals were filtered and washed thoroughly with deionized water.

The initial characterization was carried out using powder X-ray diffraction (XRD) and thermogravimetric analysis (TGA). The powder XRD pattern indicated that the products were new materials; the patterns were entirely consistent with the structures determined using the single-crystal X-ray diffraction. A least-squares fit of the powder XRD (Cu Kα) lines, using the *hkl* indices generated from single-crystal X-ray data, gave the following cell for **I**, $a = 10.149(4)$, $b = 9.951(5)$, $c = 10.399(6)$ Å, $\beta = 92.2(2)°$ and for **II**, $a = 9.279(3)$, $b = 9.724(3)$, $c = 14.297(3)$ Å, $\beta = 90.9(1)°$, which is in agreement with that determined using the single-crystal XRD. Powder data for **I**, $[C_3N_2H_{12}]_2[Zn_4(PO_4)_4]$, and **II**, $[C_3N_2H_{12}]_2[Zn_5(H_2O)(PO_4)_4(HPO_4)]$, are listed in Tables 1 and 2.

Thermogravimetric analysis (TGA) of compounds **I** and **II** were carried out in nitrogen atmosphere in the range between 25 and 700 °C (Figure 1).The TGA study indicates that the weight loss occurs in two steps for **I** and in three steps for **II**. The total mass loss of 21.34% in the case of **I** corresponds well with the loss of the amine and condensation of the phosphate (calcd 20.95%), and a mass loss of 20.3% in the case of **II** correspond with the loss of the bound water, loss of amine and condensation of the phosphate (calcd 20.8%). In both the cases, the loss of the amine molecule resulted in the collapse of the framework structure, leading to the formation of largely amorphous weakly diffracting materials (XRD) that corresponds to dense zinc phosphate phases [$Zn_2P_2O_7$, JCPDS: 34-623], consistent with the structures.

Single-Crystal Structure Determination. A suitable colorless single crystal of each compound was carefully selected under a polarizing microscope and glued to a thin glass fiber with cyanoacrylate (superglue) adhesive. Crystal structure determination by X-ray diffraction was performed on a Siemen's SMART-CCD diffractometer equipped with a normal focus, 2.4 kW sealed tube X-ray source (Mo Kα radiation, $\lambda = 0.71073$ Å) operating at 50 kV and 40 mA. A hemisphere of intensity data were collected at room temperature in 1321 frames with ω scans (width of 0.30° and exposure time of 10 s per frame) in the 2θ range 3−46.5°. Pertinent experimental details for the structure determinations of **I** and **II** are presented in Table 3.

(14) *Atlas of zeolite structure types*; Meier, W. H., Olson, D. H., Baerlocher, Ch., Eds.; Elsevier, Boston, 1996.

Table 1. X-ray Powder Data for I, $[C_3N_2H_{12}]_2[Zn_4(PO_4)_4]$

h	*k*	*l*	$2\theta_{obs}$	$\Delta(2\theta)^a$	d_{calc}	$\Delta(d)^b$	I_{rel}c
0	1	1	12.419	−0.104	7.187	−0.060	98.1
1	1	0	12.461	0.001	7.103	0.001	99.6
1	1	−1	14.934	−0.015	5.938	−0.006	7.9
1	1	1	15.396	−0.099	5.792	−0.037	6.5
0	0	2	17.114	−0.048	5.196	−0.015	14.8
2	1	0	19.653	−0.004	4.518	−0.001	15.8
1	1	−2	20.896	0.016	4.248	0.003	18.4
2	1	−1	21.204	−0.028	4.196	−0.006	17.1
1	2	−1	21.558	−0.037	4.129	−0.007	22.6
1	2	1	21.815	−0.027	4.079	−0.005	32.8
2	0	2	25.105	−0.105	3.562	−0.015	18.8
2	2	−1	26.131	0.170	3.388	0.022	22.0
2	2	1	26.828	−0.085	3.333	−0.010	16.8
0	1	3	27.220	0.040	3.271	0.005	100.0
3	1	0	27.871	0.002	3.201	0.000	74.4
1	3	0	28.304	0.003	3.153	0.001	25.3
1	1	−3	28.377	−0.013	3.147	−0.001	8.1
1	3	−1	29.558	−0.047	3.027	−0.005	7.1
2	1	−3	32.002	0.018	2.795	0.002	4.6
1	2	−3	32.502	−0.060	2.760	−0.005	29.9
3	2	−1	32.928	−0.020	2.722	−0.002	25.5
3	2	1	33.476	−0.029	2.679	−0.002	5.7
0	0	4	34.533	−0.008	2.598	−0.001	4.7
4	0	0	35.468	−0.065	2.535	−0.004	9.7
2	2	−3	35.697	0.025	2.513	0.002	5.0
0	4	0	36.149	−0.045	2.488	−0.003	6.7
4	0	1	36.751	0.057	2.442	0.004	3.1
4	1	−1	37.244	0.051	2.411	0.003	5.1
0	3	3	37.488	0.054	2.396	0.003	3.4
3	2	3	42.210	−0.042	2.143	−0.002	6.9
2	4	2	44.376	0.042	2.040	0.002	3.1
4	3	0	45.055	−0.052	2.014	−0.002	5.1
3	3	−3	45.824	0.018	1.979	0.001	3.6
4	3	1	46.080	0.082	1.966	0.003	2.9
5	1	1	46.876	−0.016	1.939	−0.001	2.9
2	5	0	49.142	0.037	1.853	0.001	8.6

[a] $2\theta_{obs} - 2\theta_{calcd}$. [b] $d_{obs} - d_{calcd}$. [c] $100 \times I/I_{max}$.

Table 2. X-ray Powder Data for II, $[C_3N_2H_{12}]_2[Zn_5(H_2O)(PO_4)_4(HPO_4)]$

h	*k*	*l*	$2\theta_{obs}$	$\Delta(2\theta)^a$	d_{calc}	$\Delta(d)^b$	I_{rel}^c
1	0	0	9.576	−0.043	9.278	−0.042	15.4
0	0	2	12.407	−0.024	7.148	−0.014	100.0
1	1	0	13.204	−0.015	6.713	−0.008	88.7
0	2	0	18.269	−0.023	4.862	−0.006	21.8
2	0	1	20.230	−0.008	4.391	−0.002	5.7
1	0	−3	20.818	−0.002	4.267	−0.001	3.1
2	1	1	22.197	0.015	4.002	0.003	11.5
2	0	−2	22.717	−0.037	3.921	−0.006	16.4
2	0	2	23.042	−0.016	3.862	−0.003	14.0
1	2	−2	24.045	−0.001	3.701	−0.000	11.6
0	0	4	24.936	−0.023	3.574	−0.003	4.9
2	2	0	26.568	−0.011	3.356	−0.001	8.6
2	2	−1	27.203	0.017	3.276	0.002	8.1
1	1	−4	28.128	0.019	3.170	0.002	33.7
1	3	0	29.175	0.008	3.060	0.001	14.9
3	0	1	29.657	−0.003	3.012	−0.000	19.2
1	3	1	29.886	0.008	2.989	0.001	23.2
0	2	4	31.046	0.010	2.880	0.001	12.1
2	0	−4	31.317	0.028	2.854	0.002	11.4
2	0	4	31.843	0.015	2.809	0.001	6.5
0	1	5	32.668	−0.022	2.743	−0.002	6.1
1	0	5	32.897	0.034	2.720	0.003	4.8
3	0	3	34.840	0.001	2.575	0.000	2.6
2	2	4	36.956	0.002	2.432	0.000	5.0
4	2	0	43.211	0.005	2.093	0.000	5.0
1	2	6	43.574	−0.024	2.078	−0.001	1.7
0	0	7	44.353	0.003	2.042	0.000	1.0

[a] $2\theta_{obs} - 2\theta_{calcd}$. [b] $d_{obs} - d_{calcd}$. [c] $100 \times I/I_{max}$.

An absorption correction based on symmetry equivalent reflections was applied using SADABS program.[15] Other effects, such as absorption by the glass fiber, were simultaneously corrected. For both **I** and **II**, the systematic absences

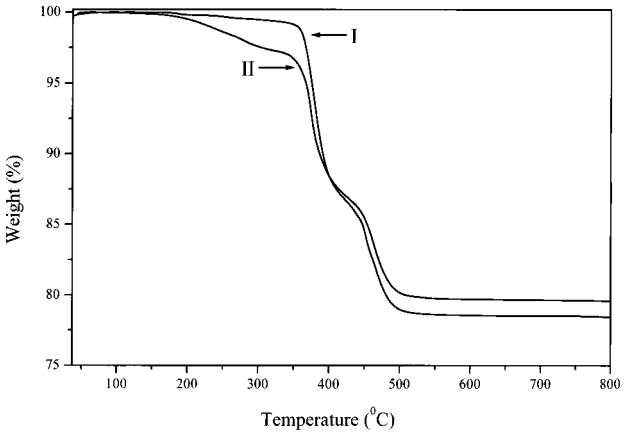

Figure 1. TGA curve for **I**, $[C_3N_2H_{12}]_2[Zn_4(PO_4)_4]$, and **II**, $[C_3N_2H_{12}]_2[Zn_5(H_2O)(PO_4)_4(HPO_4)]$ showing the weight loss.

Table 3. Summary of Crystal Data, Intensity Measurements and Structure Refinements Parameters for I, $[C_3N_2H_{12}]_2[Zn_4(PO_4)_4]$, and II, $[C_3N_2H_{12}]_2[Zn_5(H_2O)(po_4)_4(HPO_4)]$

parameter	I	II
empirical formula	$Zn_4P_4O_{16}C_6N_4H_{24}$	$Zn_5P_5O_{21}C_6N_4H_{27}$
habit	truncated octahedron	rectangular plate
crystal system	monoclinic	monoclinic
space group	$P2_1$	$P2_1$
crystal size (mm)	0.12 × 0.12 × 0.24	0.12 × 0.16 × 0.20
a (Å)	10.200(1)	9.299(4)
b (Å)	9.998(1)	9.751(1)
c (Å)	10.447(1)	14.334(1)
β (deg)	92.24(2)	90.97(4)
V (Å^3)	1064.62(3)	1299.67(9)
Z	2	2
formula mass	793.6	973.02
ρ_{calc} (g cm^{-3})	2.476	2.486
λ (Mo Kα) Å	0.71073	0.71073
μ (mm^{-1})	4.840	4.955
θ range	1.95−23.25	1.42−23.29
total data collected	4523	5438
index ranges	$-11 \le h \le 10$	$-10 \le h \le 10$
	$-11 \le k \le 7$	$-10 \le k \le 10$
	$-11 \le l \le 10$	$-15 \le l \le 8$
unique data	2253	3576
observed data $I > 2\sigma(I)$)	2231	3389
refinement method	full-matrix least-squares on $\|F^2\|$	
R_{merg}	0.07	0.03
R indexes $I > 2\sigma(I)$]	$R_1 = 0.038$[a]	$R_1 = 0.028$
	w$R_2 = 0.099$[b]	w$R_2 = 0.063$
R (all data)	$R_1 = 0.038$	$R_1 = 0.031$
	w$R_2 = 0.099$	w$R_2 = 0.064$
goodness of fit S_{obs})	1.069	1.051
no. of variables	308	379
largest difference map peak nd hole, eÅ^{-3}	1.055 and −1.074	0.423 and −0.470

[a] $R_1 = \sum ||F_0|-|F_c||/\sum |F_0|$; [b] w$R_2 = \{\cdot[w(F_0^2 - F_c^2)^2]/\cdot[w(F_0^2)^2]\}^{1/2}$. $w = 1/[\sigma^2(F_0)^2 + (aP)^2 + bP]$, $P = [\max.(F_0^2,0) + 2(F_c)^2]/3$, where $a = 0.0769$ and $b = 1.3519$ for **I** and $a = 0.0104$ and $b = 0.0$ for **II**.

in the reduced data ($0k0$, $k \neq 2n$) indicated space groups $P2_1$ or $P2_1/m$. The structures were solved by direct methods, in the polar space group $P2_1$, using SHELXS-86.[16] In each case, a sufficient fragment of the structure was revealed (Zn, P, and O) to enable the remainder of the non-hydrogen atoms to be located from difference Fourier maps and the refinements to proceed to $R < 10\%$. All the hydrogen positions were initially located in the difference map and for the final refinement the hydrogen atoms were placed geometrically and held in the

Table 4. Final Atomic Coordinates [× 10^4] and Equivalent Isotropic Displacement Parameters [Å^2 × 10^3] for I, $[C_3N_2H_{12}]_2[Zn_4(PO_4)_4]$

atom	x	y	z	U_{eq}[a]
Zn(1)	1372(1)	4235(1)	8927(1)	14(1)
Zn(2)	6276(1)	5989(1)	8789(1)	14(1)
Zn(3)	9170(1)	6501(1)	6012(1)	14(1)
Zn(4)	4208(1)	3143(1)	6250(1)	14(1)
P(1)	9282(2)	6173(2)	9058(2)	12(1)
P(2)	3841(2)	637(2)	4313(2)	11(1)
P(3)	1144(2)	3968(2)	5878(2)	12(1)
P(4)	4327(2)	3546(2)	9293(2)	13(1)
O(1)	3194(5)	4568(7)	9309(6)	28(2)
O(2)	591(5)	5973(7)	9170(5)	24(1)
O(3)	1009(5)	3448(7)	7242(5)	24(1)
O(4)	618(5)	2867(7)	9989(5)	27(2)
O(5)	4297(6)	2620(7)	10459(5)	27(1)
O(6)	5916(5)	6302(7)	6978(5)	21(1)
O(7)	5631(5)	4294(7)	9384(5)	23(1)
O(8)	8155(5)	5742(7)	9376(5)	24(1)
O(9)	7633(4)	5553(8)	5434(5)	27(2)
O(10)	10706(5)	5397(7)	5766(6)	26(1)
O(11)	9673(5)	8089(7)	5033(5)	24(1)
O(12)	9040(5)	7297(7)	7719(5)	22(1)
O(13)	5655(5)	4200(7)	5655(5)	23(1)
O(14)	4236(5)	2694(6)	8057(5)	23(1)
O(15)	2610(5)	3953(7)	5527(5)	24(1)
O(16)	4548(5)	1437(7)	5372(5)	24(1)
N(4)	7967(8)	5956(9)	2040(8)	37(2)
N(3)	7430(7)	2452(9)	4440(7)	32(2)
C(6)	8249(8)	4627(10)	2571(8)	27(2)
C(5)	6955(9)	3795(11)	2522(9)	36(2)
C(4)	7167(9)	2427(12)	3057(9)	35(2)
N(2)	6918(7)	−1049(8)	7082(7)	29(2)
N(1)	7790(9)	2679(12)	9283(8)	61(3)
C(3)	6751(8)	306(11)	7563(8)	27(2)
C(2)	8080(8)	1077(10)	7568(8)	23(2)
C(1)	7985(10)	2478(13)	7930(9)	43(3)

[a] U(eq) is defined as one-third of the trace of the orthogonalized U_{ij} tensor.

Table 5. Selected Bond Distances for I, $[C_3N_2H_{12}]_2[Zn_4(PO_4)_4]$

moiety	d (Å)	moiety	d (Å)
Zn(1)−O(1)	1.916(5)	P(1)−O(4)$^{\#1}$	1.525(6)
Zn(1)−O(2)	1.932(7)	P(1)−O(12)	1.527(5)
Zn(1)−O(4)	1.939(6)	P(1)−O(2)$^{\#2}$	1.528(6)
Zn(1)−O(3)	1.950(5)	P(1)−O(8)	1.550(6)
Zn(2)−O(5)$^{\#1}$	1.911(6)	P(2)−O(16)	1.524(6)
Zn(2)−O(7)	1.929(7)	P(2)−O(13)$^{\#3}$	1.526(7)
Zn(2)−O(6)	1.938(5)	P(2)−O(6)$^{\#3}$	1.533(5)
Zn(2)−O(8)	2.005(5)	P(2)−O(9)$^{\#3}$	1.539(5)
Zn(3)−O(9)	1.910(6)	P(3)−O(10)$^{\#4}$	1.500(7)
Zn(3)−O(10)	1.942(6)	P(3)−O(11)$^{\#3}$	1.520(6)
Zn(3)−O(12)	1.962(5)	P(3)−O(3)	1.528(6)
Zn(3)−O(11)	1.968(6)	P(3)−O(15)	1.554(5)
Zn(4)−O(13)	1.937(6)	P(4)−O(7)	1.526(6)
Zn(4)−O(14)	1.940(5)	P(4)−O(5)	1.531(6)
Zn(4)−O(15)	1.946(5)	P(4)−O(1)	1.543(6)
Zn(4)−O(16)	1.973(6)	P(4)−O(14)	1.546(6)
		Organic Moiety	
N(1)−C(1)	1.448(13)	N(3)−C(4)	1.459(12)
C(1)−C(2)	1.46(2)	C(4)−C(5)	1.49(2)
C(2)−C(3)	1.559(12)	C(5)−C(6)	1.559(13)
C(3)−N(2)	1.457(14)	C(6)−N(4)	1.464(13)

[a] Symmetry transformations used to generate equivalent atoms: #1, $-x + 1$, $y + {}^1/_2$, $-z + 2$; #2, $x + 1$, y, z; #3, $-x + 1$, $y - {}^1/_2$, $-z + 1$; #4, $x - 1$, y, z.

(15) Sheldrick, G. M. *SADABS Siemens Area Detector Absorption Correction Program*; University of Gottingen: Gottingen, Germany, 1994.

(16) Sheldrick, G. M. *SHELXS-86 Program for Crystal Structure Determination*; University of Gottingen: Gottingen, Germany, 1986; *Acta Crystallogr.* **1990**, *A35*, 467.

Table 6. Selected Bond Angles for I, $[C_3N_2H_{12}]_2[Zn_4(PO_4)_4]$[a]

moiety	angle (deg)	moiety	angle (deg)
O(1)−Zn(1)−O(2)	102.6(3)	O(4)$^{\#1}$−P(1)−O(12)	108.2(4)
O(1)−Zn(1)−O(4)	114.0(3)	O(4)$^{\#1}$−P(1)−O(2)$^{\#2}$	106.3(3)
O(2)−Zn(1)−O(4)	112.6(3)	O(12)−P(1)−O(2)$^{\#2}$	111.4(3)
O(1)−Zn(1)−O(3)	114.0(2)	O(4)$^{\#1}$−P(1)−O(8)	111.4(3)
O(2)−Zn(1)−O(3)	114.7(3)	O(12)−P(1)−O(8)	110.0(3)
O(4)−Zn(1)−O(3)	99.6(3)	O(2)$^{\#2}$−P(1)−O(8)	109.5(4)
O(5)$^{\#1}$−Zn(2)−O(7)	120.2(2)	O(16)−P(2)−O(13)$^{\#3}$	109.2(3)
O(5)$^{\#1}$−Zn(2)−O(6)	102.4(3)	O(16)−P(2)−O(6)$^{\#3}$	108.8(3)
O(7)−Zn(2)−O(6)	97.3(2)	O(13)$^{\#3}$−P(2)−O(6)$^{\#3}$	111.2(3)
O(5)$^{\#1}$−Zn(2)−O(8)	106.5(3)	O(16)−P(2)−O(9)$^{\#3}$	110.0(3)
O(7)−Zn(2)−O(8)	97.3(2)	O(13)$^{\#3}$−P(2)−O(9)$^{\#3}$	106.0(4)
O(6)−Zn(2)−O(8)	117.4(2)	O(6)$^{\#3}$−P(2)−O(9)$^{\#3}$	111.6(3)
O(9)−Zn(3)−O(10)	109.5(3)	O(10)$^{\#4}$−P(3)−O(11)$^{\#3}$	110.4(3)
O(9)−Zn(3)−O(12)	113.9(2)	O(10)$^{\#4}$−P(3)−O(3)	111.0(4)
O(10)−Zn(3)−O(12)	115.8(2)	O(11)$^{\#3}$−P(3)−O(3)	108.7(3)
O(9)−Zn(3)−O(11)	117.6(3)	O(10)$^{\#4}$−P(3)−O(15)	106.1(3)
O(10)−Zn(3)−O(11)	99.3(2)	O(11)$^{\#3}$−P(3)−O(15)	110.9(3)
O(12)−Zn(3)−O(11)	100.0(3)	O(3)−P(3)−O(15)	109.8(3)
O(13)−Zn(4)−O(14)	117.1(2)	O(7)−P(4)−O(5)	106.9(3)
O(13)−Zn(4)−O(15)	106.6(3)	O(7)−P(4)−O(1)	109.0(4)
O(14)−Zn(4)−O(15)	117.0(2)	O(5)−P(4)−O(1)	110.7(3)
O(13)−Zn(4)−O(16)	100.0(2)	O(7)−P(4)−O(14)	110.2(3)
O(14)−Zn(4)−O(16)	104.9(3)	O(5)−P(4)−O(14)	109.2(4)
O(15)−Zn(4)−O(16)	109.8(3)	O(1)−P(4)−O(14)	110.7(3)
P(4)−O(1)−Zn(1)	127.1(4)	P(2)$^{\#6}$−O(9)−Zn(3)	135.6(4)
P(1)$^{\#4}$−O(2)−Zn(1)	142.1(4)	P(3)$^{\#2}$−O(10)−Zn(3)	140.4(4)
P(3)−O(3)−Zn(1)	133.2(4)	P(3)$^{\#6}$−O(11)−Zn(3)	130.1(3)
P(1)$^{\#5}$−O(4)−Zn(1)	152.8(4)	P(1)−O(12)−Zn(3)	131.5(4)
P(4)−O(5)−Zn(2)$^{\#5}$	149.1(4)	P(2)$^{\#6}$−O(13)−Zn(4)	140.1(3)
P(2)$^{\#6}$−O(6)−Zn(2)	139.3(4)	P(4)−O(14)−Zn(4)	133.1(4)
P(4)−O(7)−Zn(2)	135.9(4)	P(3)−O(15)−Zn(4)	135.4(3)
P(1)−O(8)−Zn(2)	124.4(4)	P(2)−O(16)−Zn(4)	134.8(4)
		Organic Moiety	
N(1)−C(1)−C(2)	113.6(10)	N(3)−C(4)−C(5)	111.9(9)
C(1)−C(2)−C(3)	114.2(8)	C(4)−C(5)−C(6)	111.5(8)
C(2)−C(3)−N(2)	110.3(7)	C(5)−C(6)−N(4)	108.6(8)

[a] Symmetry transformations used to generate equivalent atoms: #1, $-x+1, y+{}^1/_2, -z+2$; #2, $x+1, y, z$; #3, $-x+1, y-{}^1/_2, -z+1$; #4, $x-1, y, z$; #5, $-x+1, y-{}^1/_2, -z+2$; #6, $-x+1, y+{}^1/_2, -z+1$.

riding mode. The Flack polarity parameter[17] was optimized to establish the absolute structure of **I** and **II**. A refined value of 0.02(1) for **I** and 0.06(1) for **II** indicated that the absolute structure is as given in the Results. Final residuals of $R_1 = 0.038$ and $wR_2 = 0.099$ for **I**, $R_1 = 0.028$ and $wR_2 = 0.063$ for **II**, respectively were obtained for refinements varying atomic positions for all the atoms and anisotropic thermal parameters for all non-hydrogen atoms and isotropic thermal parameters for all the hydrogen atoms. By setting the Flack parameter to 1.00 (opposite absolute structure) and repeating the refinement resulted in residuals of $R_1 = 0.048$ and $wR_2 = 0.14$ for **I**, $R_1 = 0.046$ and $wR_2 = 0.11$ for **II**, respectively. Since no chiral reagents were used in the synthesis, there is no reason to suspect that the bulk sample of **I** and **II** consists of anything other than a random 50:50 mixture of crystals of both absolute structures. Full-matrix-least-squares structure refinement against $|F^2|$ was carried out using the SHELXTL-PLUS[18] package of program. The final atomic coordinates, and selected bond distances and angles for **I** are presented in Tables 4−6, and for **II** in Tables 7−9.

Results

$[N_2C_3H_{12}]_2[Zn_4(PO_4)_4]$, I. The asymmetric unit of **I** contains 34 non-hydrogen atoms as shown in Figure 2,

(17) Flack, H. D. *Acta Crystallogr.* **1983**, *A39*, 876.
(18) Sheldrick, G. M. *SHELXS-93 Program for Crystal Structure Solution and Refinement*; University of Gottingen: Gottingen, Germany, 1993.

Table 7. Final Atomic Coordinates [$\times 10^4$] and Equivalent Isotropic Displacement Parameters [Å$^2 \times 10^3$] for II, $[C_3N_2H_{12}]_2[Zn_5(H_2O)(PO_4)_4(HPO_4)]$

atom	x	y	z	U_{eq}[a]
Zn(1)	−4677(1)	8853(1)	2673(1)	14(1)
Zn(2)	2284(1)	13769(1)	3755(1)	14(1)
Zn(3)	2437(1)	14040(1)	1300(1)	15(1)
Zn(4)	−706(1)	11135(1)	2456(1)	15(1)
Zn(5)	−770(1)	7396(1)	2270(1)	18(1)
P(1)	−2046(2)	9262(2)	3935(1)	13(1)
P(2)	−2438(2)	9165(2)	986(1)	14(1)
P(3)	−444(2)	14289(2)	2378(1)	11(1)
P(4)	2646(2)	11220(2)	2423(1)	13(1)
P(5)	4444(2)	15628(2)	2725(1)	12(1)
O(1)	−3718(5)	8606(6)	1506(3)	36(1)
O(2)	−3611(5)	9699(4)	3709(3)	19(1)
O(3)	−5245(5)	7045(4)	3087(3)	20(1)
O(4)	−6355(6)	10012(5)	2483(4)	37(1)
O(5)	2416(6)	11857(5)	3378(3)	26(1)
O(6)	4123(4)	14629(4)	3518(3)	19(1)
O(7)	−1834(5)	8883(6)	4955(3)	29(1)
O(8)	582(4)	14608(5)	3193(3)	23(1)
O(9)	377(4)	14074(5)	1467(3)	21(1)
O(10)	2863(5)	14401(5)	26(3)	23(1)
O(11)	3242(5)	15618(4)	1994(3)	19(1)
O(12)	3238(5)	12292(5)	1740(3)	20(1)
O(13)	−1010(5)	10443(5)	3700(3)	24(1)
O(14)	−1369(5)	13025(4)	2579(3)	20(1)
O(15)	1196(5)	10699(5)	2030(3)	22(1)
O(16)	−1940(5)	10540(5)	1425(3)	24(1)
O(17)	−1687(5)	7987(5)	3363(4)	28(1)
O(18)	1325(7)	7620(8)	2482(5)	32(2)
O(19)	−1178(5)	8135(5)	1043(3)	25(1)
O(20)	−1471(5)	5511(4)	2250(3)	19(1)
O(21)	5820(5)	15024(5)	2219(4)	27(1)
N(1)	6030(6)	2529(6)	11083(4)	23(1)
N(2)	8921(7)	5632(6)	9971(4)	31(2)
C(3)	7481(8)	4995(7)	10064(5)	24(2)
C(2)	7501(8)	3487(8)	9837(5)	29(2)
C(1)	6125(8)	2742(9)	10073(5)	31(2)
N(3)	3783(6)	7535(6)	6152(4)	25(1)
N(4)	981(6)	10844(6)	5232(4)	25(1)
C(7)	2336(8)	10094(8)	5269(6)	31(2)
C(6)	2144(8)	8623(8)	4968(5)	34(2)
C(5)	3464(9)	7751(9)	5144(5)	36(2)

[a] U(eq) is defined as one-third of the trace of the orthogonalized U_{ij} tensor.

of which 24 atoms belong to the "framework" and 10 atoms to the "guest" species. There are four crystallographically distinct Zn and P atoms. The zinc atoms are tetrahedrally coordinated by their O atom neighbors with Zn−O bond lengths in the range 1.910−2.005 Å (av. Zn(1)−O = 1.934, Zn(2)−O = 1.945, Zn(3)−O = 1.946, Zn(4)−O = 1.949 Å). The O−Zn−O angles are in the range 97.3−120.2° (av. O−Zn(1)−O = 109.6, O−Zn(2)−O = 109.6, O−Zn(3)−O = 109.4, O−Zn(4)−O = 109.2°). The four zinc atoms make four Zn−O−P bonds to four distinct P atom neighbors with a fairly wide spread of angles and an average Zn−O−P bond angle of 136.6°. The phosphorus atoms also make four P−O−Zn linkages. The P−O distances are in the range 1.500−1.554 Å (av. P(1)−O = 1.533, P(2)−O = 1.531, P(3)−O = 1.526, P(4)−O = 1.537 Å) and the O−P−O bond angles are in the range 106−1−111.6° (av. 109.5°). Assuming the usual valence of Zn, P, and O to be +2, +5, and −2 respectively, the framework stoichiometry of $Zn_4(PO_4)_4$ creates a net framework charge of −4. The presence of two molecules of $[NH_3(CH_2)_3NH_3]$ would account for +4 arising from the complete protonation of the amine. Bond valence sum calculations[19] on the framework agree with the above results.

Table 8. Selected Bond Distances for II, $[C_3N_2H_{12}]_2[Zn_5(H_2O)(PO_4)_4(HPO_4)]$[a]

moiety	*d* (Å)	moiety	*d* (Å)
Zn(1)−O(1)	1.924(4)	P(1)−O(7)	1.517(5)
Zn(1)−O(2)	1.954(5)	P(1)−O(17)	1.529(5)
Zn(1)−O(3)	1.936(4)	P(1)−O(13)	1.542(5)
Zn(1)−O(4)	1.942(5)	P(1)−O(2)	1.545(5)
Zn(2)−O(5)	1.946(5)	P(2)−O(10)$^{\#2}$	1.515(5)
Zn(2)−O(6)	1.940(4)	P(2)−O(1)	1.516(5)
Zn(2)−O(7)$^{\#1}$	1.907(4)	P(2)−O(19)	1.544(4)
Zn(2)−O(8)	1.944(4)	P(2)−O(16)	1.548(5)
Zn(3)−O(9)	1.934(4)	P(3)−O(8)	1.527(5)
Zn(3)−O(10)	1.908(4)	P(3)−O(14)	1.533(4)
Zn(3)−O(11)	1.974(4)	P(3)−O(20)$^{\#3}$	1.536(5)
Zn(3)−O(12)	1.960(5)	P(3)−O(9)	1.539(4)
Zn(4)−O(13)	1.933(5)	P(4)−O(4)$^{\#4}$	1.501(5)
Zn(4)−O(14)	1.952(4)	P(4)−O(5)	1.522(5)
Zn(4)−O(15)	1.928(4)	P(4)−O(15)	1.539(5)
Zn(4)−O(16)	1.945(5)	P(4)−O(12)	1.540(5)
Zn(5)−O(17)	1.886(5)	P(5)−O(3)$^{\#5}$	1.502(5)
Zn(5)−O(18)	1.978(7)	P(5)−O(11)	1.520(5)
Zn(5)−O(19)	1.933(5)	P(5)−O(6)	1.530(5)
Zn(5)−O(20)	1.951(4)	P(5)−O(21)	1.595(4)
	Organic Moiety		
C(1)−C(2)	1.515(10)	C(4)−C(5)	1.511(11)
C(2)−C(3)	1.506(10)	C(5)−C(6)	1.508(11)
C(3)−N(2)	1.484(9)	C(6)−N(4)	1.457(9)

[a] Symmetry transformations used to generated equivalent atoms: #1, $-x, y + 1/2, -z + 1$; #2, $-x, y - 1/2, -z$; #3, $x, y + 1, z$; #4, $x + 1, y, z$; #5, $x + 1, y + 1, z$.

The framework structure of **I**, is built from strictly alternating ZnO_4 and PO_4 tetrahedra that are linked through their vertices giving rise to the three-dimensional architecture possessing channels. The connectivity between ZnO_4 and PO_4 tetrahedra results in four-membered rings, which are connected to each other via oxygens. The connectivity between the four-membered rings is such that they are arranged around the 2-fold screw axis forming a chain as shown in Figure 3. The chains are further connected together within and out of the plane forming eight-membered helical channels along *a* axis (Figure 4). The width of this channel is 9.1 × 5.6 Å. The structure can also be visualized to result from the connectivity involving the double crankshaft chains as shown in Figure 5. The double crankshaft chains, employing Liebau notation,[20] are useful in describing the zeolitic structures. The connectivity between such crankshaft chains results in a one-dimensional channel in **I** (Figure 5). Along the *c* axis, the connectivity between the tetrahedra gives rise to another eight-membred channels of width 6.7 × 6.5 Å as shown in Figure 6. The structure directing amine molecule, diprotonated DAP molecule, sits in the middle of these channels and interact with the framework through hydrogen bonds (Figure 7). The important hydrogen-bond distances are presented in Table 10.

$[C_3N_2H_{12}]_2[Zn_5(H_2O)(PO_4)_4(HPO_4)]$, II. The asymmetric unit contains 41 non-hydrogen atoms as shown in Figure 8 with five Zn and P atoms being crystallographically distinct. The structure consists of strictly alternating ZnO_4, PO_4 and HPO_4 tetrahedra connected through Zn−O−P bonds, giving rise to the three-

Table 9. Selected Bond Angles for II, $[C_3N_2H_{12}]_2[Zn_5(H_2O)(PO_4)_4(HPO_4)]$[a]

moiety	angle (deg)	moiety	angle (deg)
O(1)−Zn(1)−O(3)	106.6(2)	O(7)−P(1)−O(17)	107.0(3)
O(1)−Zn(1)−O(4)	109.5(2)	O(7)−P(1)−O(13)	108.7(3)
O(3)−Zn(1)−O(4)	110.5(2)	O(17)−P(1)−O(13)	110.3(3)
O(1)−Zn(1)−O(2)	118.5(2)	O(7)−P(1)−O(2)	112.1(3)
O(3)−Zn(1)−O(2)	106.8(2)	O(17)−P(1)−O(2)	109.0(3)
O(4)−Zn(1)−O(2)	104.9(2)	O(13)−P(1)−O(2)	109.8(3)
O(7)$^{\#1}$−Zn(2)−O(6)	110.7(2)	O(10)$^{\#2}$−P(2)−O(1)	109.3(3)
O(7)$^{\#1}$−Zn(2)−O(8)	100.8(2)	O(10)$^{\#2}$−P(2)−O(19)	109.5(3)
O(6)−Zn(2)−O(8)	117.4(2)	O(1)−P(2)−O(19)	110.0(3)
O(7)$^{\#1}$−Zn(2)−O(5)	109.9(2)	O(10)$^{\#2}$−P(2)−O(16)	109.2(3)
O(6)−Zn(2)−O(5)	107.8(2)	O(1)−P(2)−O(16)	110.1(3)
O(8)−Zn(2)−O(5)	110.1(2)	O(19)−P(2)−O(16)	108.7(3)
O(10)−Zn(3)−O(9)	109.7(2)	O(8)−P(3)−O(14)	111.4(3)
O(10)−Zn(3)−O(12)	112.6(2)	O(8)−P(3)−O(20)$^{\#3}$	108.2(3)
O(9)−Zn(3)−O(12)	110.3(2)	O(14)−P(3)−O(20)$^{\#3}$	107.2(2)
O(10)−Zn(3)−O(11)	104.8(2)	O(8)−P(3)−O(9)	111.3(2)
O(9)−Zn(3)−O(11)	107.0(2)	O(14)−P(3)−O(9)	109.7(3)
O(12)−Zn(3)−O(11)	112.1(2)	O(20)$^{\#3}$−P(3)−O(9)	108.7(3)
O(15)−Zn(4)−O(13)	111.4(2)	O(4)$^{\#4}$−P(4)−O(5)	111.4(3)
O(15)−Zn(4)−O(13)	111.4(2)	O(4)$^{\#4}$−P(4)−O(15)	107.4(3)
O(15)−Zn(4)−O(16)	103.1(2)	O(5)−P(4)−O(15)	109.2(3)
O(15)−Zn(4)−O(16)	103.1(2)	O(4)$^{\#4}$−P(4)−O(12)	110.0(3)
O(13)−Zn(4)−O(14)	101.3(2)	O(5)−P(4)−O(12)	110.6(3)
O(16)−Zn(4)−O(14)	99.6(2)	O(15)−P(4)−O(12)	108.2(3)
O(17)−Zn(5)−O(19)	123.9(2)	O(3)$^{\#5}$−P(5)−O(11)	112.3(3)
O(17)−Zn(5)−O(20)	98.3(2)	O(3)$^{\#5}$−P(5)−O(6)	111.6(3)
O(19)−Zn(5)−O(20)	106.1(2)	O(11)−P(5)−O(6)	111.0(2)
O(17)−Zn(5)−O(18)	107.3(3)	O(3)$^{\#5}$−P(5)−O(21)	110.2(3)
O(19)−Zn(5)−O(18)	106.1(3)	O(11)−P(5)−O(21)	105.6(3)
O(20)−Zn(5)−O(18)	115.7(3)	O(6)−P(5)−O(21)	105.7(3)
P(2)−O(1)−Zn(1)	139.6(3)	P(5)−O(11)−Zn(3)	128.4(3)
P(1)−O(2)−Zn(1)	120.5(3)	P(4)−O(12)−Zn(3)	131.1(3)
P(5)$^{\#6}$−O(3)−Zn(1)	141.6(3)	P(1)−O(13)−Zn(4)	124.3(3)
P(4)$^{\#7}$−O(4)−Zn(1)	163.6(4)	P(3)−O(14)−Zn(4)	124.2(2)
P(4)−O(5)−Zn(2)	130.7(3)	P(4)−O(15)−Zn(4)	127.9(3)
P(5)−O(6)−Zn(2)	126.0(3)	P(2)−O(16)−Zn(4)	137.3(3)
P(1)−O(7)−Zn(2)$^{\#8}$	157.2(3)	P(1)−O(17)−Zn(5)	143.1(3)
P(3)−O(8)−Zn(2)	136.5(3)	P(2)−O(19)−Zn(5)	115.3(3)
P(3)−O(9)−Zn(3)	127.9(3)	P(3)$^{\#10}$−O(20)−Zn(5)	121.5(3)
P(2)$^{\#9}$−O(10)−Zn(3)	146.5(3)		
		Organic Moiety	
N(1)−C(1)−C(2)	110.7(6)	N(3)−C(4)−C(5)	113.0(6)
C(1)−C(2)−C(3)	114.0(6)	C(4)−C(5)−C(6)	113.3(7)
C(2)−C(3)−N(2)	112.0(6)	C(5)−C(6)−N(4)	111.6(6)

[a] Symmetry transformations used to generated equivalent atoms: #1, $-x, y + 1/2, -z + 1$; #2, $-x, y - 1/2, -z$; #3, $x, y + 1, z$; #4, $x + 1, y, z$; #5, $x + 1, y + 1, z$; #6, $x - 1, y - 1, z$; #7, $x - 1, y, z$; #8, $-x, y - 1/2, -z + 1$; #9, $-x, y + 1/2, -z$; #10, $x, y - 1, z$.

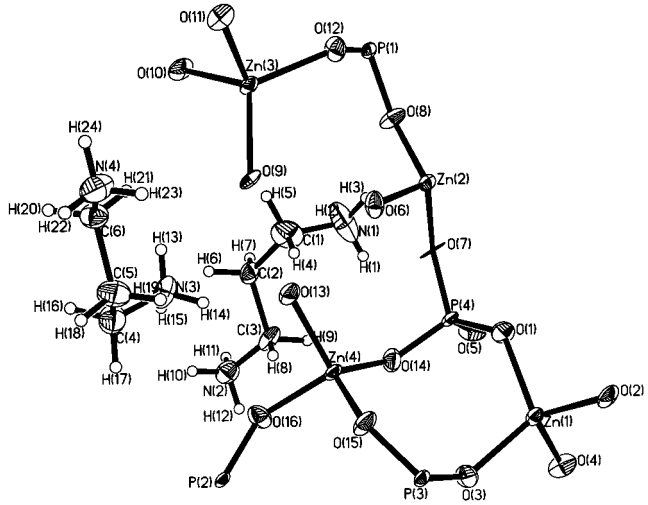

Figure 2. ORTEP plot of **I**, $[C_3N_2H_{12}]_2[Zn_4(PO_4)_4]$. Thermal ellipsoids are given at 50% probability.

(19) Brown, I. D.; Aldermatt, D. *Acta Crystallogr., Sect. B* **1984**, *41*, 244.

(20) (a) Liebau, F. *Structural Chemistry of Silicates. Structure, bonding and classification*; Springer: Berlin, 1985. (b) Liebau, F. *Zeolites* **1983**, *3*, 191.

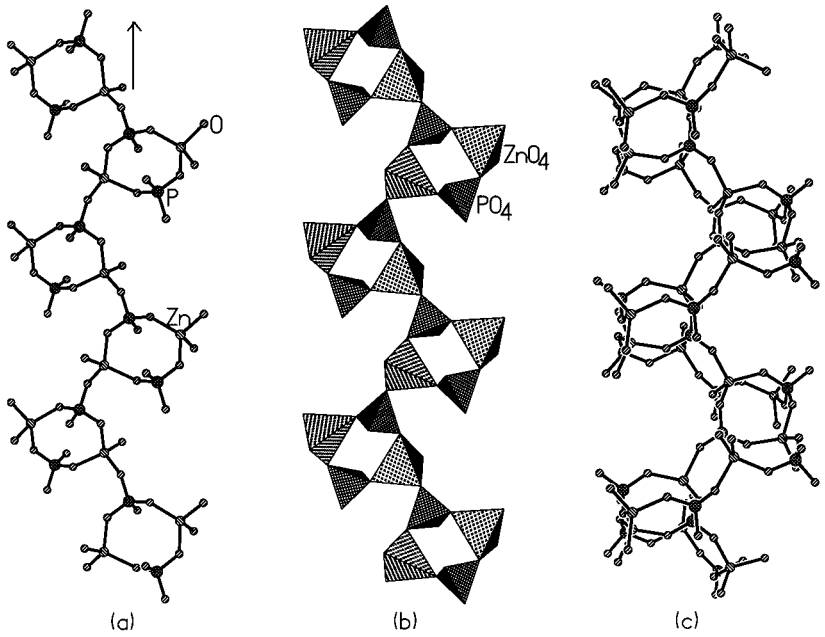

Figure 3. (a) The chainlike structure formed by the connectivity between the four-membered rings, in **I**. Arrow indicates the 2-fold screw axis formed along the *c* axis. (b) Polyhedral representation showing the linkages between the four-membered rings. (c) Connectivity between two such chains along the *c* axis.

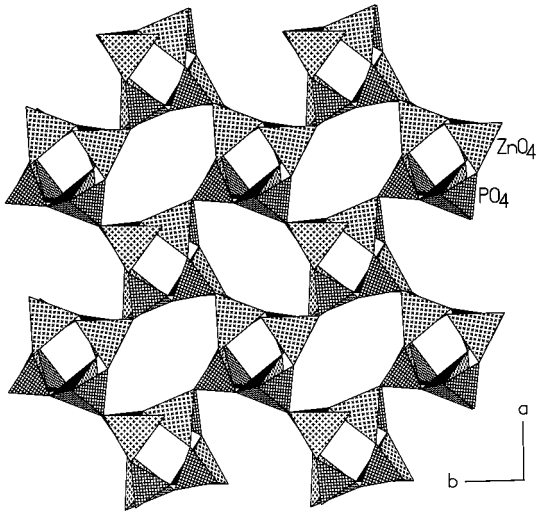

Figure 4. Polyhedral view of **I** along [001] axis. Note that the connectivity creates a eight-membered channels. The amine molecule occupies these channels (not shown).

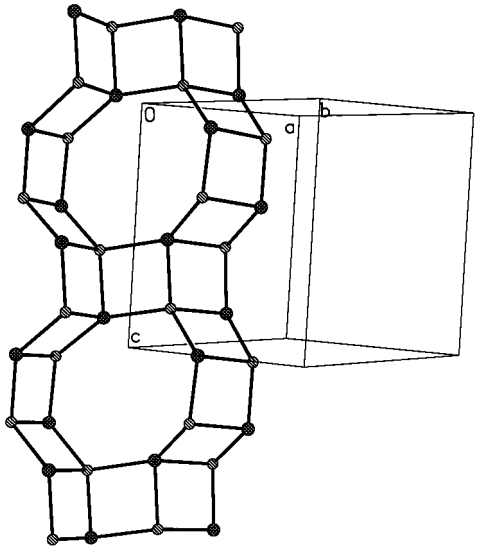

Figure 5. The double crankshaft chains in **I**. Note the connectivity between the chains form a eight-membered channel.

dimensional architecture. The Zn atoms are all tetrahedrally coordinated to four oxygen atoms with the Zn−O bond length in the range 1.886−1.978 Å (av. 1.939 Å). The O−Zn−O bond angles are in the range 98.3−123.9° (av. 109.5°). Of the five independent Zn atoms, one zinc [Zn(5)] atom makes three Zn−O−P linkages and possess a terminal Zn−O bond and the remaining Zn atoms make four Zn−O−P linkages, resulting in an average bond angle of 128.4° for such a connectivity. Similarly, P(5) makes only three P−O−Zn linkages with one terminal P−O bond, and the remaining P atoms make four P−O−Zn bonds. The P−O bond distances are in the range 1.501−1.595 Å (av. 1.532 Å) and the O−P−O angles are in the range 105.6−112.3° (av. 109.5°). These geometrical parameters are in good agreement with those reported for similar compounds in the literature.[4−13] The framework structure of $Zn_5O(PO_4)_5$ would result in a net framework charge of −7. The presence of two molecules of $[NH_3(CH_2)_3NH_3]$ would account for +4 charge arising from the diprotonation of the amine. The excess negative charge of −3 is then needed to be balanced. Bond valence sum calculations[19] indicate that P(5)−O(21) with a distance of 1.595 Å is formally a −OH group and Zn(5)−O(18) with a distance of 1.978 Å is a water molecule, which also corresponds well with the proton positions located in the difference Fourier maps. Formation of terminal water molecules linked to Zn centers have been known to occur in open-framework zinc phosphates.[10a]

The ZnO_4, PO_4, and HPO_4 tetrahedra are linked to each other, forming four-membered rings which are connected variably forming the secondary building unit (SBU) as shown in Figure 9. Similar SBU has been

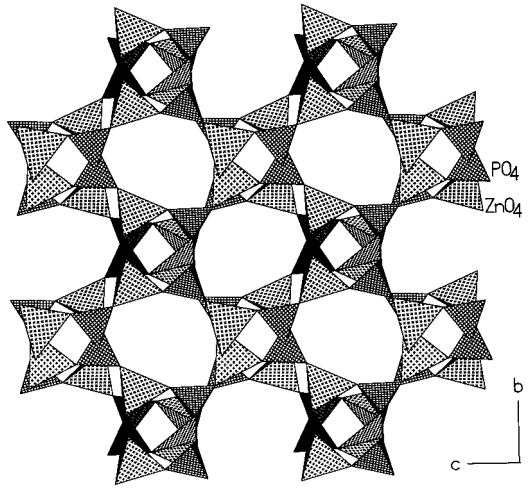

Figure 6. Polyhedral view of **I** along the [100] axis showing the eight-membered channels.

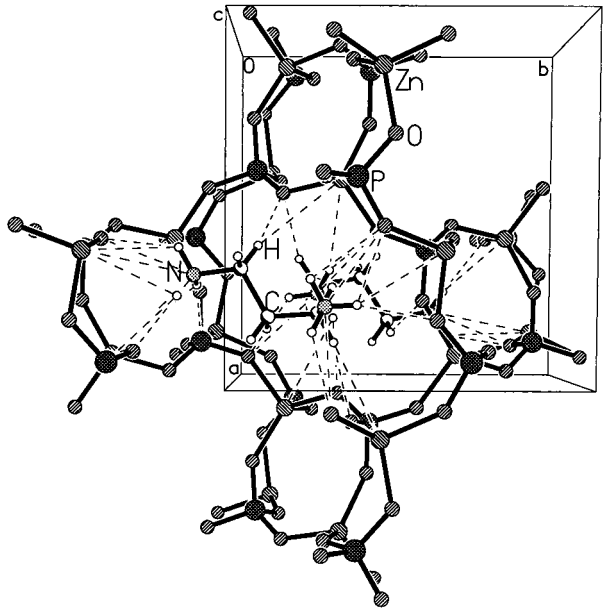

Figure 7. Structure of **I** showing a single eight-membered channel along with the amine. Dotted lines represent the various hydrogen bond interactions.

observed for the aluminosilicate, thomsonite. The SBUs are connected so as to form a dimeric unit, which are linked together forming the structure. The presence of a terminal water molecule and a −OH group creates interruptions in the connectivity of the SBUs in **II**, that the total structure is marginally different than that of thomsonite. The SBUs are connected and arranged around the 2-fold screw axis (Figure 9). It is interesting to note that the SBU has close resemblance to the building units found in NASICON type structures[21] as shown in Figure 10. The central portion of the SBU in **II** is built up from three PO_4 tetrahedra capped by two ZnO_4 tetrahedra, unlike in $NaZr_2(PO_4)_3$, where the phosphate units are capped by two octahedra forming a lantern-like arrangement. In $NaZr_2(PO_4)_3$, the lanterns are so connected as to form channels wherein the Na ions are located. In **II**, the SBUs are connected to each other, forming channels along the *a* axis as shown in Figures 11 and 12. These channels are bound by eight T atoms (T = Zn, P), and have width of 6.7 × 5.9 Å along the *a* axis. The position of the amine molecules within the channels, along the *a* axis, is such that they replicate the 2-fold screw axis as shown in Figure 11.

(21) Hong, H. *Mater. Res. Bull.* **1976**, *11*, 173 and references therein.

Table 10. Selected Hydrogen-Bond Interactions in I and II

moiety	*d* (Å)	moiety	angle (deg)
	Compound **I**		
O(2)−H(2)	1.997(1)	O92)−H92)−N(1)	156.5(3)
O(8)−H(3)	2.233(1)	O(8)−H(3)−N(1)	160.4(1)
O(15)−H(10)	1.912(2)	O(15)−H(10)−N(2)	166.8(2)
O(12)−H(11)	1.988(1)	O(12)−H(11)−N(2)	148.3(2)
O(11)−H(13)	2.244(2)	O(11)−H913)−N(3)	150.8(2)
O(13)−H(14)	1.999(2)	O(13)−H(14)−N(3)	159.4(1)
O(8)−H(22)	2.027(2)	O(8)−H(22)−N(4)	145.4(2)
O(3)−H(5)	2.396(2)	O(3)−H(5)−C(1)	163.9(2)
O(16)−H(8)	2.395(2)	O(16)−H(8)−C(3)	165.5(3)
O(1)−H(9)	2.483(3)	O(1)−H99)−C(3)	148.5(2)
O(6)−H(17)	2.439(2)	O(6)−H(17)−C(4)	154.1(2)
O(7)−H(18)	2.593(2)	O(7)−H(18)−C(5)	163.0(1)
	Compound **II**		
O(16)−H(1)	1.971(2)	O(16)−H(1)−N(1)	160.2(2)
O(21)−H(2)	2.037(2)	O(21)−H(2)−N(1)	169.1(2)
O(12)−H(3)	1.996(2)	O(12)−H(3)−N(1)	144.3(2)
O(9)−H(10)	2.064(2)	O(9)−H(10)−N(2)	161.2(2)
O(15)−H(11)	2.050(1)	O(15)−H(11)−N(2)	149.1(2)
O(19)−H(12)	2.049(3)	O(19)−H(12)−N(2)	152.4(2)
O(13)−H(22)	2.046(2)	O(13)−H(22)−N(4)	156.8(3)
O(8)−H(23)	2.086(3)	O(8)−H(23)−N(4)	161.6(2)
O(7)−H(24)	2.268(4)	O(7)−H(24)−N(4)	148.4(2)
O(17)−H(24)	2.193(2)	O(17)−H(24)−N(4)	142.7(3)
N(1)−H(30)	2.170(2)	O(21)−H(30)−O(21)	151.4(4)
O(11)−H(51)[a]	1.924(4)	O(11)−H(51)−O(18)[a]	160.6(2)
O(15)−H(52)[a]	2.593(2)	O(15)−H(52)−O(18)[a]	151.7(2)
O(1)−H(5)	2.432(2)	O(1)−H(5)−C(1)	141.8(3)
O(10)−H(5)	2.521(2)	O910)−H(5)−C(1)	154.0(1)
O(21)−H(8)	2.509(3)	O(21)−H(8)−C(3)	165.5(2)

[a] Intralayer.

Discussion

Two new three-dimensional open-framework zinc phosphates, **I**, $[C_3N_2H_{12}]_2[Zn_4(PO_4)_4]$, and **II**, $[C_3N_2H_{12}]_2[Zn_5(H_2O)(PO_4)_4(HPO_4)]$, have been obtained as good quality single crystals by hydrothermal methods. Although the structures of both **I** and **II** are formed from the expected tetrahedral building blocks of ZnO_4 and PO_4 units, sharing vertices, distinct differences exist between them. The syntheses of both the compounds were effected by minor variations in the synthesis mixture. The unpredictable nature of the kinetically controlled solvent-mediated reactions is well-illustrated by the formation of two different phases by the small variation in the reaction mixture. As is typical of such reactions, there is no correlation between the starting composition and the majority solid-phase product.

Compounds **I** and **II** consist of three-dimensional networks with Zn−O−P bonds strongly favored over possible Zn−O−Zn or P−O−P linkages. This may be largely due to the Zn:P ratio of 1:1, which is rather unusual as most of the zinc phosphates have Zn: P ratio > 1.0. The difficulty in obtaining a zinc phosphate structure with Zn:P ratio of 1:1, with Zn and P atoms fully ordered, as in the present case, is in packing enough bulky organic cations into the extra-framework pores to achieve the charge balance. It is to be noted that, despite the Zn:P ratio of 1:1 in **I** and **II**, there are no terminal P−OH linkages in the compounds (except

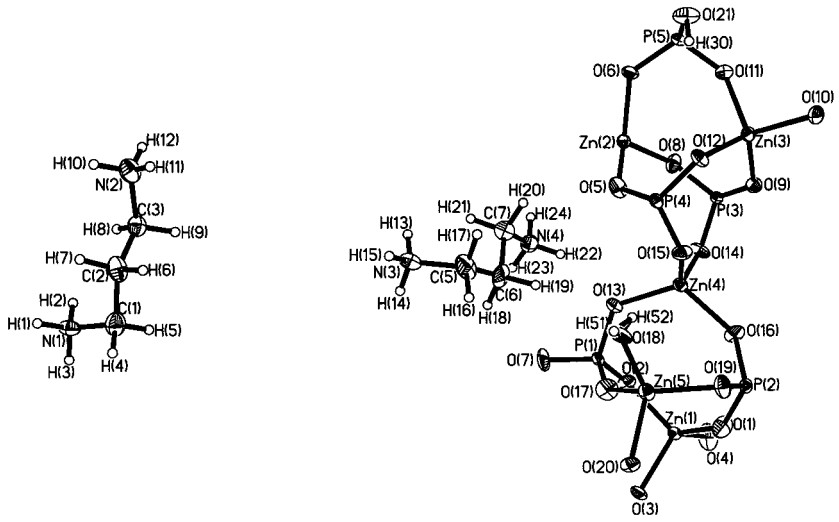

Figure 8. ORTEP plot of **II**, $[C_3N_2H_{12}]_2[Zn_5(H_2O)(PO_4)_4(HPO_4)]$. The thermal ellipsoids are given at 50% of the probability.

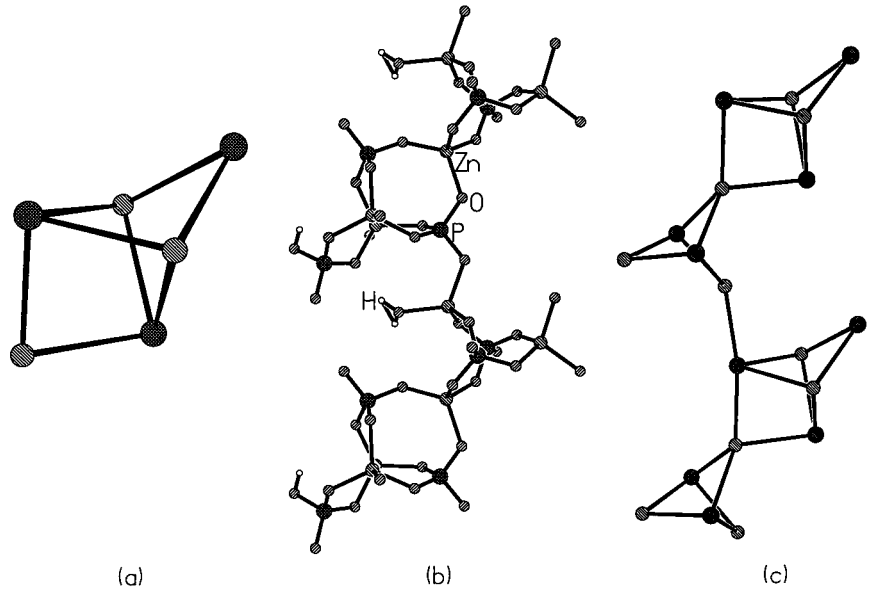

Figure 9. (a) The secondary building unit (SBU) present in **II**. Only the T atom (T = Zn, P) connectivity is given. Similar SBU has been observed for thomsonite (see text). (b) The connectivity between the SBUs that forms a chainlike arrangement around the 2-fold screw axis. (c) The T atom connectivity showing the same.

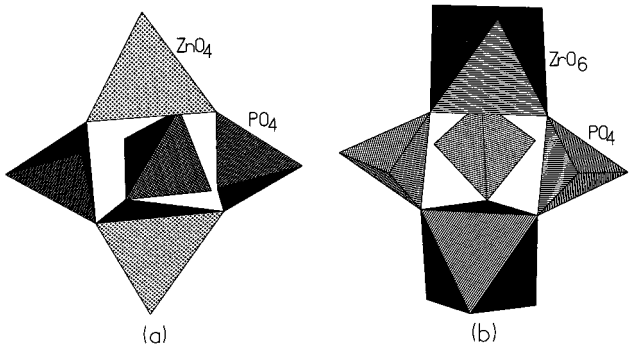

Figure 10. (a) Polyhedral connectivity of the building unit in **II**. (b) Polyhedral connectivity of the building units in NASICON-type compounds. Note the similarity between the two.

in **II**, which possess a single P−OH bond). The formation of framework protons or P−OH-type linkages arise in these materials essentially to obtain charge neutrality. In the present materials, the fact that the framework is built up from 1:1 tetrahedral arrangement of Zn and P atoms, suggest indirectly that the organic cations, which is linear, are arranged in such a way that they charge balance the framework. Such zinc phosphate structures without terminal P−OH bonds have been detailed in the literature and are usually templated by alkali metals.[9b,c]

It is important to ponder over the formation of **I** and **II**, which are prepared by employing similar synthesis conditions, but formed with dissimilar structures, despite having an identical Zn/P ratio of 1.0. It is to be noted that the structures of **I** and **II** are formed by TO_4 tetrahedra (T = Zn, P), and the individual tetrahedra are more or less regular (Tables 5 and 8). But the average T−O−T bond angles are quite different in the both cases (Tables 6 and 9); while the Zn−O−P bond angle is 136.6° in **I**, it is 128.4° in **II**. Such differences in the bond angles may be responsible for the variations in the two structures observed in the present study. In the case of aluminosilicates, where the structures are made from AlO_4 and SiO_4 tetrahedra, the individual

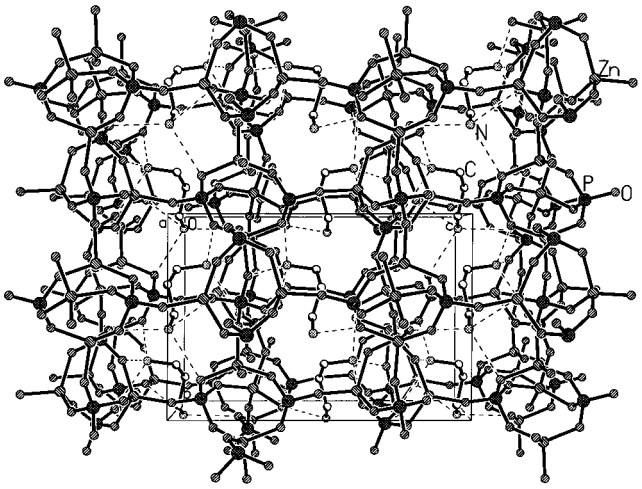

Figure 11. Structure of **II** along the *a* axis showing the eight-membered channels and the position of the amine. Note the amine is arranged so as to replicate the screw axis. Dotted lines represents the various hydrogen bond interactions. Hydrogens are not shown for clarity.

tetrahedra are close to being regular (109.5°), but the T−O−T bond angles can accommodate values ranging from ∼125° to 180°. The variations in the bond angles have been hypothesized as one of the reasons for the occurrence of many zeolitic structures, despite having similar Si/Al ratios.[14]

In addition to the above, unlike in many of the aluminosilicates, where the framework charges are generally matched with that of the templates by variations in the Si:Al ratio, with only a minor change in the framework topology, the zinc phosphates seem to have precisely defined Zn:P ratio for a particular topology. The resulting charge imbalance caused by the fixed Zn:P ratio, is usually compensated by the presence of phosphate units that are variably protonated. This limits our ability to change the framework charge distribution to match that of the template without significantly altering the framework structure. In the case of **II**, however, the presence of a terminal water molecule and a monohydrogen phosphate (HPO_4) group helps in maintaining the charge neutrality and in the process, giving rise to a completely different structure than that of **I**.

The "openness" of a structure is defined in terms of the tetrahedral atom density[14] (framework density, FD), defined as the number of tetrahedral (T) atoms per 1000 Å^3. In the present materials, the number of T atoms per 1000 Å^3 (here T = Zn and P) are 15 and 15.4 for **I** and **II**, respectively. These values are in the middle of the range of FD values observed in aluminosilicate zeolites, where the presence of channels is common. The FD value of 15.4 observed for **II** is between 17.7 and 14.4 T/1000 Å^3, which is the value for the normal thomsonite and the expanded one.[14]

It is well-known that multipoint hydrogen bond interactions are necessary in the formation and stability of open architectures. In the present case also, we find strong hydrogen-bond interactions involving the hydrogens attached to the nitrogen of the amine and the framework oxygen atoms. The terminal water molecule and −OH group, in the case of **II**, in addition to the hydrogens attached to the carbon atoms also participate in hydrogen bonds. The majority of the interactions are quite strong as indicated by the short hydrogen-acceptor distances (∼2.2 Å) and a donor−hydrogen−acceptor angle of ∼150°. The important hydrogen-bond interactions for **I** and **II** are presented in Table 10.

It is instructive to compare the various zinc phosphates that have been prepared using the same amine, DAP. Harrison et al.[6c] reported zinc phosphates with ladder and layer architectures by the use of DAP.

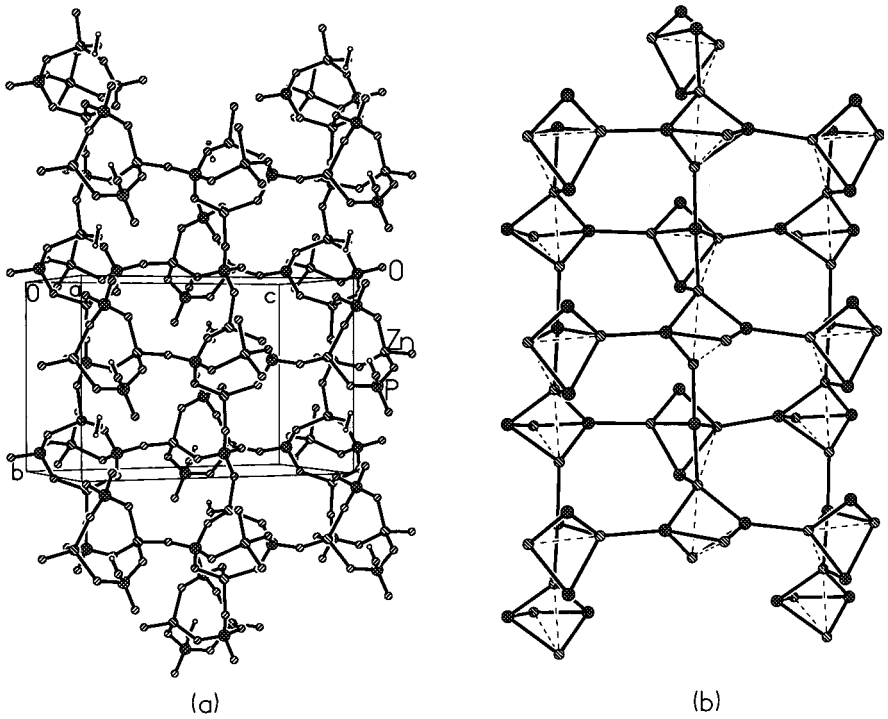

Figure 12. (a) Ball and stick view of the structure of **II** along the *c* axis showing the connectivity between the one-dimensional chains that form the channels. The amine molecules are not shown. (b) The T atom connectivity showing the channels. Note the interrupted connectivity between the SBUs (see text).

Recently, studies in this laboratory has shown that the use of DAP results in the formation of a three-dimensional structure, wherein the amine molecule performs a dual role—that of a structure-directing agent and a ligand.[13b] In the present case, we have obtained two different three-dimensional structures possessing channels, one of them **II** is closely related to the mineral, thomsonite. One of the reasons for the observed three-dimensional structure might be the choice of reagents used in the synthesis. The synthesis of **I** and **II** have been effected by the addition of acetic acid in the medium, in addition to hydrochloric acid. It is likely that the Cl^- ions might just be acting as a mineralizer similar to the F^- ions in some of the synthesis of the phosphates of Al and Ga.[22] The role of acetic acid in the formation of **I** and **II** is not clear. It is likely that the acetate ions, present in the mixture during the synthesis, might act as a base and favor the deprotonation of H_3PO_4. The fact that the final products in both **I** and **II** are essentially formed by the PO_4 units (completely deprotonated H_3PO_4) lends credence to this argument. In this connection, it is to be noted that a three-dimensional zinc phosphate has been prepared with DAP, by using oxalic acid as an additive.[13b] It is possible that the oxalate ions performs a role similar to the acetate ions in the present synthesis—that of deprotonation of the phosphoric acid. The ladder and layer structures formed by DAP[6c] possess HPO_4 and H_2PO_4 moieties. To validate such an assumption, we sought to prepare compounds **I** and **II** using zinc acetate instead of ZnO in the starting mixture. As expected, pure phases of **I** and **II** were obtained in the preparations. In addition, we have employed several organic mono- and diacids as additives in the synthesis of zinc phosphates, which invariably resulted in the formation of zinc phosphates possessing completely deprotonated PO_4 units. It is appears that by deprotonating the phosphoric acid, mono- and dicarboxylic acids help in maintaining the pH of the reaction mixture, which is crucial in the synthesis of open-framework phosphate materials.

(22) Chippindale, A. M.; Natarajan, S.; Thomas, J. M.; Jones, R. H. *J. Solid State Chem*. **1994**, *111*, 18 and references therein.

Conclusions

Hydrothermal synthesis of two new open-framework zinc phosphates, **I**, $[C_3N_2H_{12}]_2[Zn_4(PO_4)_4]$, and **II**, $[C_3N_2H_{12}]_2[Zn_5(H_2O)(PO_4)_4(HPO_4)]$, has been accomplished using the same organic amine, 1,3-diaminopropane. The structures of **I** and **II** have three-dimensional architectures possessing channels arising from the vertex linkages involving ZnO_4, PO_4, and HPO_4 tetrahedra. It is interesting that a minor variation in the starting composition gives rise to two completely different structures, indicating that the two structures have comparable energies. Further studies are necessary to understand the role of acetate ions and of minor compositional changes in yielding different open-framework structures.

Acknowledgment. The authors thank Professor C. N. R. Rao, FRS for his kind help, support, and encouragement.

Supporting Information Available: X-ray crystallographic data for compounds I and II. This material is available free of charge via the Internet at http://pubs.acs.org.

CM000283U